Far-infrared resonance spectroscopy and the effective intermolecular potential

M. W. Evans
Department of Physics, University College of North Wales, Bangor, Gwynedd, Wales, United Kingdom
(Received 25 September 1984)

The Kramers equation is solved numerically for circular diffusion in an arbitrary periodic potential $V(\theta)$, where θ is the angular coordinate. In the limit $\beta \rightarrow 0$, where β becomes proportional to the rate of escape from the potential wells, the far-infrared power absorption coefficient shows *many different peaks* due to resonance in highly nonlinear systems as described by Bogoliubov and Mitropolsky for ordinary, nonlinear, differential equations. The far-infrared resonance spectrum (FIRRS) is sensitive to the details of V. In structured (associated or hydrogen-bonded) molecular liquids such as water or acetonitrile, or in liquid crystals, the FIRRS peaks *can be resolved experimentally.* These peaks provide, in principle, detailed information on the effective intermolecular potential in systems of interest such as nematogens. The FIRRS spectrum is sensitive to an applied, uniaxial, external, static, electric or magnetic field.

INTRODUCTION

There have been numerous attempts[1–5] at solving numerically the Kramers equation governing molecular diffusion in liquids and similar rate processes. The first useful solution was given by Reid[6] for diffusion in a cosine potential of the form:

$$V = -V_0 \cos[M\theta(t)] \tag{1}$$

where V_0 is the effective well depth, M the well multiplicity, and $\theta(t)$ the angular coordinate for circular diffusion. In this paper the solution is extended to deal with arbitrary potential $V(\theta)$, given in general by a Fourier series. In principle, the details of $V(\theta)$ may be synthesized from a sum of terms such as (1) using, as a guide, the results of self-consistent field molecular orbital computation of real intermolecular potentials in the liquid state.

These details may be compared with experimental data using the numerical finding by Evans[7] that the far-infrared spectrum predicted by the Kramers equation *becomes structured with resonance peaks* in the limit $\beta \rightarrow 0$, when β becomes proportional to the rate of escape from potential wells [of type (1) in the simplest case]. The existence of this far-infrared resonance spectrum (FIRRS) was first observed by Evans *et al.*[8] and has been confirmed recently by Evans in liquid water[9] and in associated liquids such as acetonitrile[10] and nitromethane.[9] These peaks are shown in this paper to have a firm foundation in the theory of nonlinear, differential equations, described, for example, by Bogoliubov and Mitropolsky.[11] The peaks from the *stochastic,* partial-differential Kramers equation vary greatly[12] in relative frequency and intensity with parameters such as

(i) $\alpha = (kT/I)^{1/2}$, where I is the effective molecular moment of inertia;

(ii) β, the rate of escape from the potential wells;

(iii) the well-depth parameter γ, defined by Reid[6] as $\gamma = V_0/2(IkT)^{1/2}$;

(iv) the multiplicity M.

This paper is arranged as follows. The theory for arbitrary $V(\theta)$ is developed in Sec. I, followed by a discussion of the numerical results in Sec. II. Section III finally suggests the way to proceed when using FIRRS to estimate experimentally the effective intermolecular potential in, for example, water, or an aligned nematogen such as 4-cyano-4-(n-heptyl) biphenyl (7 CB).

I. THEORY

The Kramers equation for circular diffusion in a potential $V(\theta)$ may be written, in the simplest case, as

$$\frac{\partial \rho}{\partial t} + \dot{\theta}\frac{\partial \rho}{\partial \theta} - \frac{V'}{I}\frac{\partial \rho}{\partial \dot{\theta}} = \beta \frac{\partial}{\partial \dot{\theta}}\left[\dot{\theta}\rho + \frac{kT}{I}\frac{\partial \rho}{\partial \dot{\theta}}\right] . \tag{2}$$

Here $\rho(\dot{\theta}(t),\theta(t),t \mid \dot{\theta}(0),\theta(0),0)$ is the conditional probability density function in the phase space of $\dot{\theta}$ and θ. Equation (2) is fully equivalent[13] to the Langevin equation:

$$I\ddot{\theta}(t) + I\beta\dot{\theta}(t) + V'(\theta) = \dot{W}(t) , \tag{3}$$

where $W(t)$ is a Wiener process.[14] In these equations V' denotes differentiation with respect to θ. Paradoxically, the apparently much simpler Eq. (3) has no known method of solution (without recourse to a random-number generator), while Eq. (2) may be solved numerically, using the methods of differential-difference algebra. The solution of Eq. (2) takes the general form[14]

$$\rho = \exp\left[-\frac{\dot{\theta}^2}{4\alpha^2}\right]\sum_n D_n(\dot{\theta}/\alpha)\phi(\theta,t) , \tag{4}$$

where

$$D_n(\theta) = \exp(\tfrac{1}{4}\theta^2)(-1)^n \frac{d^n}{d\theta^n}[\exp(-\tfrac{1}{2}\theta^2)]$$

are the Hermite polynomials, with the orthogonality property

$$\int_{-\infty}^{\infty} D_n(\theta)D_m(\theta)d\theta = \begin{cases} n!(2\pi)^{1/2}, & m=n \\ 0, & m\neq n \end{cases}.$$

Defining $D_n^e(\theta)=D_n\exp(\frac{1}{4}\theta^2)$, the recurrence relations follow:

$$\begin{aligned} &(D_n^e)''(\theta)=\theta(D_n^e)'-nD_n^e , \\ &D_{n+1}^e=\theta D_n^e-nD_{n-1}^e , \\ &(D_n^e)'=nD_{n-1}^e . \end{aligned} \tag{5}$$

From (4)

$$\begin{aligned} \frac{\partial\rho}{\partial\theta} &= \exp\left[-\frac{\dot\theta^2}{2\alpha^2}\right]\sum_n D_n^e\frac{\partial\phi}{\partial\theta} , \\ \frac{\partial\rho}{\partial t} &= \exp\left[-\frac{\dot\theta^2}{2\alpha^2}\right]\sum_n D_n^e\dot\phi_n , \\ \frac{\partial\rho}{\partial\dot\theta} &= \exp\left[-\frac{\dot\theta^2}{2\alpha^2}\right]\sum_n \phi_n\left[\frac{(D_n^e)'}{\alpha}-\frac{\dot\theta}{\alpha^2}D_n^e\right] , \\ \frac{\partial^2\rho}{\partial\dot\theta^2} &= \exp\left[-\frac{\dot\theta^2}{2\alpha^2}\right]\sum_n \phi_n\left[\frac{(D_n^e)''}{\alpha^2}-\frac{D_n^e}{\alpha^2}-\frac{\dot\theta}{\alpha^3}(D_n^e)'\right. \\ &\qquad \left.-\frac{\dot\theta}{\alpha^2}\left[\frac{(D_n^e)'}{\alpha}-\frac{\dot\theta}{\alpha^2}D_n^e\right]\right], \end{aligned} \tag{6}$$

and, therefore, in (2),

$$\sum_n D_n^e\dot\phi+\alpha\sum_n\left[\frac{\dot\theta}{\alpha}D_n^e\right]\frac{\partial\phi_n}{\partial\theta}-\frac{V'}{I\alpha}\sum_n\left[(D_n^e)'-\frac{\dot\theta}{\alpha}D_n^e\right] =\beta\sum_n\phi_n\left[(D_n^e)''-\frac{\dot\theta}{\alpha}(D_n^e)'\right] . \tag{7}$$

In Eqs. (5), with the argument $(\dot\theta/\alpha)$ instead of θ,

$$\sum_n D_n^e\dot\phi_n+\alpha\sum_n(D_{n+1}^e+nD_{n-1}^e)\frac{\partial\phi_n}{\partial\theta}+\frac{V'}{I\alpha}\sum_n D_{n+1}^e\phi_n =\beta\sum_n\phi_n nD_n^e . \tag{8}$$

Multiply by D_m^e and integrate with respect to $\dot\theta(t)$. The orthogonality property then gives

$$\dot\phi_m+\alpha\left[\frac{\partial\phi_{m-1}}{\partial\theta}+(m+1)\frac{\partial\phi_{m+1}}{\partial\theta}\right] +\frac{V'}{I\alpha}\phi_{m-1}+\beta m\phi_m=0 . \tag{9}$$

The functions $\phi_n(\theta,t)$ are periodic in θ, and can therefore be represented in general by a Fourier series:

$$\phi_n(\theta,t)=\sum_p A_p^n(t)\exp(ip\theta) , \quad p=0,\pm1,\ldots,\pm\infty . \tag{10}$$

Similarly, the potential term V is periodic in θ, and can also be synthesized by a truncated Fourier series. For example,

$$\begin{aligned} V &= -V_0\{\cos\theta(t)+\cos[2\theta(t)]+\cos[3\theta(t)] \\ &\qquad +\cdots+\cos[M\theta(t)]\} \\ &= -\frac{V_0}{2}\sum_M(e^{iM\theta}+e^{-iM\theta}) \end{aligned} \tag{11}$$

or

$$\begin{aligned} V &= -V_0\left[\cos\theta(t)+\frac{\cos[2\theta(t)]}{4}+\frac{\cos[3\theta(t)]}{9}\right. \\ &\qquad \left.+\cdots+\frac{\cos[M\theta(t)]}{M^2}\right] \\ &= -\frac{V_0}{2}\sum_M(e^{iM\theta}+e^{-iM\theta})/M^2 . \end{aligned} \tag{12}$$

Equation (10) in (9), gives, for the simple case,

$$V=-\frac{V_0}{2}(e^{iM\theta}-e^{-iM\theta}) ,$$

$$\sum_p e^{ip\theta}\dot A_p^m(t)+\sum_p\alpha ip[A_p^{m-1}(t)+(m+1)A_p^{m+1}(t)]e^{ip\theta}-i\gamma\sum_p[A_{r-M}^{m-1}(t)-A_{r+M}^{m-1}(t)]+\beta m\sum_p A_r^m(t)=0 . \tag{13}$$

The problem is reduced, therefore, to solving this infinite set of linear differential equations with appropriate initial conditions $A_r^m(0)$. Multiplying Eq. (13) by $e^{-ir\theta}$ and using the orthogonality property,

$$\int_{-\pi}^{\pi} e^{ip\theta}e^{-ir\theta}d\theta = \begin{cases} 2\pi & \text{if } p=r, \\ 0 & \text{if } p\neq r , \end{cases} \tag{14}$$

we obtain

$$\dot A_r^m(t)+i\alpha r[A_r^{m-1}(t)+(m+1)A_r^{m+1}(t)]-i\gamma M[A_{r-M}^{m-1}(t)-A_{r+M}^{m-1}(t)]+\beta m A_r^m(t)=0 . \tag{15}$$

In the more general case of a potential of the form (11) Eq. (15) becomes

$$\begin{aligned} \dot A_r^m(t)+\alpha ir[A_r^{m-1}(t)+(m+1)A_r^{m+1}(t)]-i\gamma[A_{r-1}^{m-1}(t)-A_{r+1}^{m-1}(t)]-2i\gamma[A_{r-2}^{m-1}(t)-A_{r+2}^{m-1}(t)] \\ -3i\gamma[A_{r-3}^{m-1}(t)-A_{r+3}^{m-1}(t)]-4i\gamma[A_{r-4}^{m-1}(t)-A_{r+4}^{m-1}(t)]-\cdots+\beta m A_r^m(t)=0 . \end{aligned} \tag{16}$$

It is possible to construct differential-difference equations of the type (15) or (16) *for any sums or differences of cosines used to synthesize the periodic potential $V(\theta)$.* The indices r and m are governed by the definitions (10) and (4), respectively. The upper index of the A_r^m functions *cannot be negative,* but the lower index takes integer values $0, \pm 1, \pm 2, \pm 3, \ldots$ to infinity.

To construct the FIRRS spectrum from equations such as (15) or (16) requires Laplace transformation as discussed by Reid.[6] The Laplace transform of Eq. (16) is

$$sA_r^m(s)-A_r^m(0)+\beta m A_r^m(s)+ip\alpha[A_r^{m-1}(s)+(m+1)A_r^{m+1}(s)]-i\gamma[A_{r-1}^{m-1}(s)-A_{r+1}^{m-1}(s)]$$
$$-2i\gamma[A_{r-2}^{m-1}(s)-A_{r+2}^{m-1}(s)]-3i\gamma[A_{r-3}^{m-1}(s)-A_{r+3}^{m-1}(s)]-4i\gamma[A_{r-4}^{m-1}(s)-A_{r+4}^{m-1}(s)]-\cdots=0 .$$

This can be rewritten as a simple matrix equation:

$$\mathbf{M}\mathbf{A}(s)=\mathbf{A}(0) . \tag{17}$$

The matrix $\mathbf{M}$ is truncated for solution. The column vector $\mathbf{A}(0)$ is the vector of initial values; arranged in the order[4]

$$\ldots A_{-r}^0(0); A_{-r+1}^0(0); \ldots; A_0^0(0); \ldots, A_{r-1}^0(0) ;$$
$$A_r^0(0); \ldots; A_{-r}^1(0); A_{-r+1}^1(0); \ldots; A_0^1(0); \ldots ;$$
$$A_{r-1}^1(0); A_r^1(0); \ldots .$$

The frequency dependence of the A coefficients is obtained therefore by inverting $\mathbf{M}$ in Eq. (16). In this paper this is achieved with Crout factorization and partial pivoting, with extended precision arithmetic for the inner products on the CDC 7600 and Cyber 205 computers, using the Numerical Algorithms Group (NAG) routine F04ADF. However, it is clear that $\mathbf{M}$ is a complex, banded, tridiagonal matrix. The process of inversion could therefore be speeded up with routines designed especially for matrices such as these. It is clear also that adding cosine terms to the potential $V(\theta)$ "thickens" the γ diagonal band, leaving the other two diagonals unaffected. Efficient routines, by the Pisa group, are discussed in Ref. 15.

The $A_r^m(s)$ coefficients are related to the far-infrared spectrum through the appropriate equilibrium autocorrelation function (ACF). The first step in the calculation is to evaluate the equilibrium orientational ACF:[14]

$$\langle \cos\theta(t)\cos\theta(0)\rangle_{\text{eq}} ,$$

subject to thermodynamic equilibrium initial conditions. At a given phase point $(\dot\theta(0),\theta(0))$

$$\langle \cos\theta(t)\cos\theta(0)\rangle_\delta=\cos\theta(0)\int\int\rho(t)\cos\theta(t)d\theta(t)d\dot\theta(t)$$
$$=(2\pi)^{1/2}\alpha\cos\theta(0)\int_{-\pi}^{\pi}\sum_p e^{-ip\theta(t)}\cos\theta(t)A_p^0(t)d\theta(t)$$
$$=\frac{(2\pi)^{3/2}}{2}\alpha\cos\theta(0)[A_1^0(t)+A_{-1}^0(t)] . \tag{18}$$

If the initial phase points $(\dot\theta(0),\theta(0))$ are distributed according to the Maxwell-Boltzmann law, then

$$\langle\langle \cos\theta(t)\cos\theta(0)\rangle_s\rangle=\langle\cos\theta(t)\cos\theta(0)\rangle_{\text{eq}}$$
$$=\frac{(2\pi)^{3/2}}{2}\alpha[\langle\cos\theta(0)A_1^0(t)\rangle+\langle\cos\theta(0)A_{-1}^0(t)\rangle] , \tag{19}$$

where

$$\langle\cos\theta(0)A_r^m(0)\rangle=\frac{1}{n!(2\pi)^{3/2}}\int\int\cos\theta(0)\exp\left[-\frac{\dot\theta(0)^2}{2\alpha^2}+\frac{2\gamma}{\alpha}\sum_M\cos[M\theta(0)]\right]D_n^e\left[\frac{\dot\theta(0)}{\alpha}\right]e^{-ir\theta(t)}d\dot\theta(0)d\theta(0) . \tag{20}$$

In Eq. (20), $\sum_M\cos[M\theta(0)]$ is meant to denote a truncated cosine sum for the potential energy $V(\theta)$ [e.g., Eqs. (11) or (12)]. From Eq. (20) it is clear that

$$\langle\cos\theta(0)A_r^m(0)\rangle=0, \quad n\neq 0 .$$

This is an important simplification of the problem of solving Eq. (17) for $A_1^0(t)$ and $A_{-1}^0(t)$ subject to the initial conditions (20).

Equation (20) simplifies to

$$\langle \cos\theta(0) A_r^0(0) \rangle = \frac{1}{2\pi} \int_{-\pi}^{\pi} \cos\theta(0) \cos[r\theta(0)] \exp\left[2 \left[\frac{\gamma}{\alpha} \right] \sum_M \cos[M\theta(0)] \right] d\theta(0)$$

$$- \frac{i}{2\pi} \int_{-\pi}^{\pi} \sin\theta(0) \cos[r\theta(0)] \exp\left[2 \left[\frac{\gamma}{\alpha} \right] \sum_M \cos[M\theta(0)] \right] d\theta(0) .$$

These initial conditions are computed in this paper for all r with numerical quadrature, the NAG routine D01GAF. This checks that the second integral in the above equation is zero to about four decimal places for all the cosine sums used in this work. The numerical uncertainty in the above equation from D01GAF is at most one part in 10^3, sometimes as small as one part in 10^6 or 10^7.

The far-infrared spectrum is obtained approximately from $\langle \cos\theta(t)\cos\theta(0) \rangle$ through the second derivative:[14]

$$-\frac{d^2}{dt^2} \langle \cos\theta(t)\cos\theta(0) \rangle_{\text{eq}} = \left\langle \frac{d}{dt} \cos\theta(t) \left[\frac{d}{dt} \cos\theta(t) \right]_{t=0} \right\rangle_{\text{eq}}$$

the rotational velocity correlation function. This is related by Fourier transformation to the far-infrared (FIR) power absorption $\alpha(\bar{\nu})$ $[\bar{\nu}=\omega/(2\pi c)]$. The one-sided Fourier transform may be carried out using the fact that it is equivalent to a Laplace transform, and therefore by using the relation $s=i\omega$ between the Laplace variable s and angular frequency ω. In general,

$$\mathcal{L}_a \left[-\frac{d^2}{dt^2} f(t) \right] = -s^2 f(s) + sf(0) + f'(0) .$$

In our case, by a property of equilibrium autocorrelation functions,

$$f'(0) = \left[\frac{d}{dt} \langle \cos\theta(t)\cos\theta(0) \rangle \right]_{t=0} = 0 .$$

Therefore, the expression for the FIR power absorption becomes

$$\alpha(\omega) \propto -s^2 \mathcal{L}_a \langle \cos\theta(t)\cos\theta(0) \rangle_{\text{eq}} + s \langle \cos^2\theta(0) \rangle_{\text{eq}} ,$$
$$\text{Re}[\alpha(\omega)] \propto \omega^2 \mathcal{L}_a \langle \cos\theta(t)\cos\theta(0) \rangle_{\text{eq}} . \quad (21)$$

Equation (21) links the far-infrared power absorption to the Kramers Eq. (2). The constant of proportionality in Eq. (21) involves the complication of the internal field, irrelevant to the present paper. A full discussion is provided in Ref. (14). Finally, the dielectric loss[14] $\epsilon''(\omega)$ is given by

$$\epsilon''(\omega) \propto \omega \mathcal{L}_a \langle \cos\theta(t)\cos\theta(0) \rangle_{\text{eq}} . \quad (22)$$

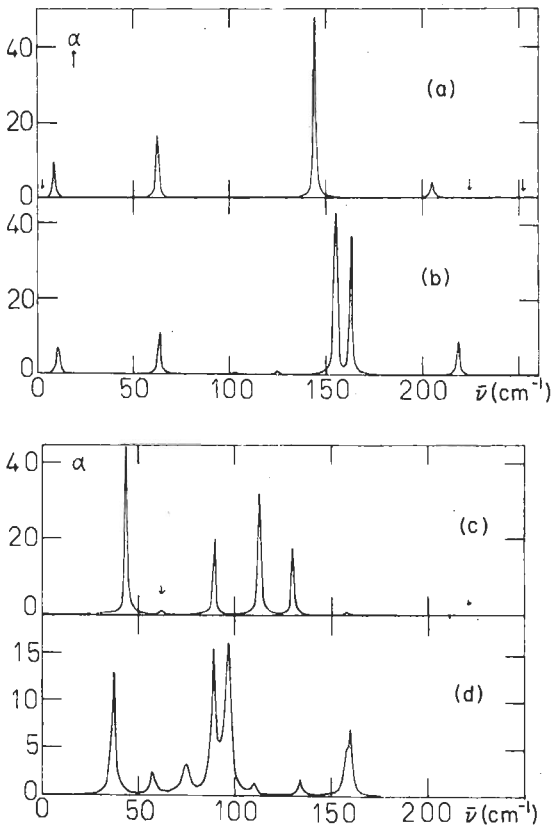

FIG. 1. FIRRS spectrum from Eq. (16), $\alpha=8$ THz; $\beta=0.1$ THz; $\gamma=5$ THz. (a),(b),(c) 100×100 matrix for V as in text. (d) 200×200 matrix.

II. NUMERICAL RESULTS

This section provides illustrations of $\text{Re}[\alpha(\bar{\nu})]$ from Eqs. (16)—(21) for various $V(\theta)$. The purpose is to evaluate the effect on the far infrared spectrum of changes in the effective intermolecular potential energy V. Checks for convergence of the solution of matrix Eq. (17) to the true solution of Eq. (2) are illustrated using various sizes of $M(s)$ in Eq. (17), 100×100 and 200×200 matrices. The parameters α, β, and γ are kept constant as $V(\theta)$ is varied, so that a direct assessment is possible of the influence of the angular dependence of the effective intermolecular potential on the far-infrared power absorption. The aim of this is to provide a new method of estimating the effective intermolecular potential in a molecular liquid or liquid crystal by fitting theoretically the observed FIRRS peaks, such as those in water.[9] The appearance of the peaks illustrated in Fig. 1, for example, is also *intrinsically* interesting, and may have new physical implications in several disciplines where nonlinear stochastic processes are considered—for example, the theory of chemical reaction rates and multiphoton processes in solution.[15]

Figure 1 illustrates $\alpha(\bar{\nu})$ for the parameters $\alpha=8$ THz, $\beta=0.1$ THz, $\gamma=5$ THz. The intermolecular potentials are as follows:

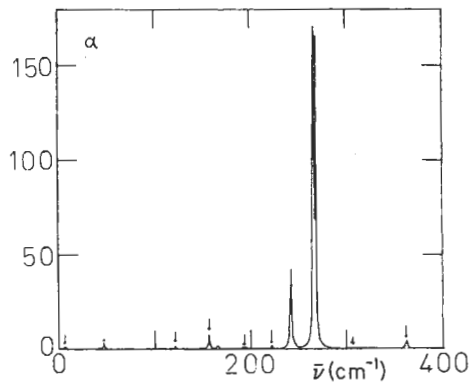

FIG. 2. As for Fig. 1; parameters as in text.

$$V=-V_0\cos[2\theta(t)]\,, \tag{23a}$$

$$V=-V_0\{\cos\theta(t)+\cos[2\theta(t)]\}\,, \tag{23b}$$

$$V=-V_0\left\{\cos\theta(t)+\frac{\cos[2\theta(t)]}{4}+\frac{\cos[3\theta(t)]}{9}+\frac{\cos[4\theta(t)]}{16}\right\}. \tag{23c}$$

The size of **M** in Eq. (16) is kept at 100×100 in Figs. 1(a)–1(c) for the purposes of direct comparison. In Fig. 1(d) the size is increased to 200×200 to illustrate the effect of convergence to the true solution of Eq. (2) for $\alpha(\bar{\nu})$. This is at the expense of an eightfold increase in computer time.

Comparing Figs. 1(a) and 1(b), it is clear that there are more FIRRS peaks for potential (23b). The potential energy of an applied electric field takes the form $V=-(\mu E/kT)\cos\theta(t)$, where μ is the molecular dipole moment and E the applied electric field strength. Therefore the effect of an external electric field **E** on the FIRRS spectrum is to create more peaks. This has been reported in the experimental literature for 7CB [4-cyano-4′-(n-heptyl) biphenyl] (Ref. 8), and acetonitrile. These preliminary experimental investigations are supported by the theory of this paper. The spectrum in Fig. 1(a) is fairly "harmonic" in nature, i.e., the peaks on the low-frequency side are separated by *approximately* equal intervals. The peaks on the low-frequency side are the more intense. Again this corroborates the preliminary experimental data[8–10] of Evans, notably in water[9] and acetonitrile.[10] The simple FIRRS spectrum of Fig. 1(a) becomes clearly anharmonic in Fig. 1(b) where seven peaks are visible for a relatively small 100×100 matrix, dominated by a doublet at about 160 cm^{-1}. It may be significant in this context that recent work by G. J. Evans, in cooperation with Nicolet Development Laboratories,[9] *has produced eight clear peaks in liquid water in the region 160 to 240 cm^{-1} alone:* at 161 cm^{-1}, 168 cm^{-1}, 173 cm^{-1}, 191 cm^{-1}, 198 cm^{-1}, 210 cm^{-1}, 221 cm^{-1}, and 232 cm^{-1}. It is hardly necessary to mention that liquid water is highly structured due to H bonding. The molecules are locked for relatively long periods in potential wells. Escape is possible only by breaking H bonds. Generalized Kramers theory [reduced model theory (RMT)] has been applied to H-bond dynamics by Grigolini *et al.*[15] The Kramers rate β is expected, therefore, to be small in liquid water. Equation (2), with the correct potential $V(\theta)$, should therefore produce FIRRS peaks in the region 160–240 cm^{-1}. This provides us with a new means of looking at H-bond dynamics in liquid water and similar media.

The more complicated potential of Fig. 1(c) shifts the whole FIRRS profile to lower frequency, again for a 100×100 matrix. *The FIRRS spectrum is therefore sensitive to changes in $V(\theta)$.* The more accurate, but much more time consuming, calculation for Fig. 1(d) (200×200 complex matrix inversion), shifts the peaks around slightly in relative frequency and intensity, but, importantly, produces *more* of them. The necessity for using very large matrices can be bypassed by resorting to fast and efficient continued-fraction solutions[5,15] of generalized Kramers equations developed by Grigolini and co-workers, and this will be the subject of future work aimed at obtaining fully converged solutions to Eq. (2) and complete FIRRS spectra for a given $V(\theta)$.

It is interesting to see that in Fig. 2, for $\alpha=8.0$ THz (moment of inertia approximately that of water) the FIRRS spectrum is dominated, for a 100×100 matrix and $V=-V_0\{\cos\theta(t)+\cos[2\theta(t)]\}$ by three intense peaks at about 250 cm^{-1}, in the region of the experimental peaks in water noted already.[9] There are already 12 peaks (Fig. 2) in the theoretical FIRRS spectrum altogether ($\gamma=10$ THz, $\beta=0.1$ THz, solid line), even for a matrix as small as 100×100.

In Fig. 3, finally, still for a small 100×100 matrix, a series of FIRRS spectra from Eq. (16) is illustrated for $\alpha=4$ THz; $\beta=0.1$ THz, $\gamma=5$ THz:

(a) $V=-V_0\{\cos\theta(t)+\cos[2\theta(t)]\}$,

(b) $V=-V_0\left\{\cos\theta(t)+\frac{\cos[2\theta(t)]}{4}+\frac{\cos[3\theta(t)]}{9}+\frac{\cos[4\theta(t)]}{16}\right\}$,

(c) $V=-V_0\left\{\cos\theta(t)+\frac{\cos[2\theta(t)]}{4}+\cdots+\frac{\cos[8\theta(t)]}{64}\right\}$,

(d) $V=-V_0\left\{\cos\theta(t)+\frac{\cos[2\theta(t)]}{4}+\cdots+\frac{\cos[12\theta(t)]}{144}\right\}$,

(e) $V=-V_0\left\{\cos\theta(t)-\frac{\cos[2\theta(t)]}{4}+\frac{\cos[3\theta(t)]}{9}-\cdots-\frac{\cos[8\theta(t)]}{64}\right\}$.

The spectra are "underdeveloped" because of the small matrix used, but it is clear that the FIRRS peaks from

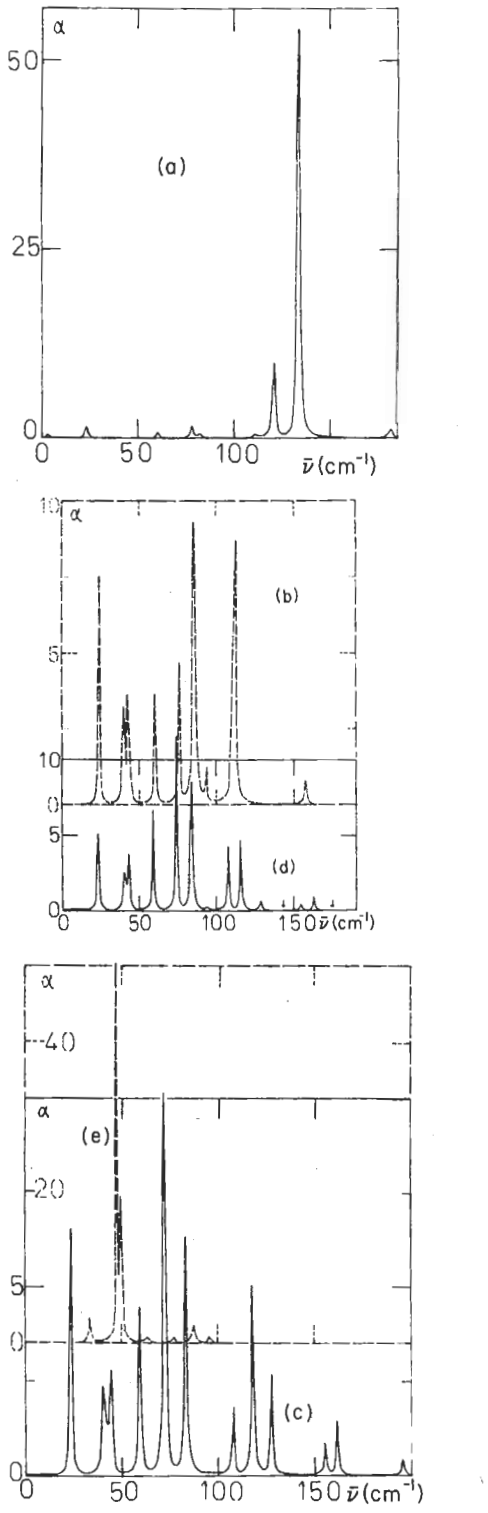

FIG. 3. As for Fig. 1; parameters as in text.

Eq. (17) vary greatly in relative intensity with the type of potential used. The peak intensity shifts to lower frequency with increasing the number of terms, the peaks of greatest intensity being concentrated on the low-frequency side, with the exception of the simple cases (a) and (e), where the truncated Fourier-series terms are alternatively positive and negative.

Provided these peaks can be resolved experimentally, by choosing the appropriate conditions, they will provide a detailed fingerprint of the effective intermolecular potential $V(\theta)$, especially in associated molecular liquids and liquid crystals.[8]

III. DISCUSSION

It is clearly important to develop a method for reducing numerically the intermolecular potential from *ab initio* quantum calculations to a form where it could be synthesized by a Fourier series and used in a Kramers equation akin to (2). The other area of development needed at present is a practical method for solving Eq. (2) in three dimensions, using all three Euler angles (θ, ϕ, and χ) rather than θ alone. It would then become possible to consider the correlation between molecular rotation and translation, which appears in the laboratory frame[16] in the presence of a parity-breaking force field.[5,14,15]

There is a growing amount of *experimental* evidence available now to suggest that *the far-infrared power absorption of molecular liquids is a broad band only when the parameter β is relatively big, i.e., when the rate of escape from potential wells is on the average rapid.* (It has been shown elsewhere[17] that the individual theoretical peaks of Figs. 1—3, for example, merge together into a broad band as β is increased.) In nematic 7CB, aligned with an electric field, the FIRRS spectrum has been resolved experimentally.[8] The FIRRS peaks are clearly visible in liquid water,[9] in liquid nitromethane,[9] and in liquid acetonitrile aligned with an electric field.[10] The so-called "rattling modes," visible in small molecules trapped in β quinol clathrates and observed in the far infrared by Davies,[18] can also be described in principle by a Kramers equation with $\beta \rightarrow 0$. In disordered solids such as the hexa-substituted benzenes,[15] separate far-infrared peaks are resolved, together with a broad dielectric loss curve at lower frequencies. [The Kramers equation (2) produces a broad $\epsilon''(\omega)$-vs-$\log_{10}\omega$ curve at low frequencies, superimposed on which are the higher frequency far-infrared resonance peaks.]

More generally, it is now known that generalized Kramers equations and master equations govern rate processes in a range of disciplines,[15] the principle being that any development in one area (such as the appearance of FIRRS peaks) might have real physical significance in another area where there is interaction between nonlinear potentials and stochastic terms in the governing rate equation. The principal feature is that *when one removes linear approximations* (e.g., $\sin\theta = \theta$) in these equations some wholly new phenomena emerge from the subsequent analysis and solution. One well known result[15] is the description of multiphoton processes by Bloembergen, using a rate equation based on nonlinear mechanics. This will be the subject of future work, based on our analysis of FIRRS peaks. Another is the self-ordering process induced by the interaction of nonlinearity and noise. The resonance peaks of this paper surely have significance in the theory of chemical reactions in solution, where the dynamical processes are selective, i.e., reaction takes place only when two molecules or ions approach in the correct trajectory, i.e., when the potential well structure is correct.[15]

Finally, we surmise, what would be the equivalent of FIRRS peaks in the stochastic rate processes of population genetics, or the theory of evolution? These processes are again governed by equations similar to (2). The same is true for stochastic processes in galactic dynamics, and in a growing number of other disciplines.

Note added in proof. The nature of these few infrared peaks has been investigated further by Grigolini and co-workers, using the Mori continued fraction[15] for the Duffing oscillator. In the limit $\beta \rightarrow 0$, the Kramers equation for the Duffing potential produces transitions corresponding to absorption peaks at regularly spaced intervals:

$$2\alpha_0, 3\alpha_0, 4\alpha_0, 5\alpha_0, \ldots ,$$

where

$$\alpha_0 = \frac{3}{4}\frac{\beta}{\omega_0^3}kT$$

with ω_0 as the natural harmonic frequency of the Duffing oscillator. Careful resummation of the Mori series leads to the conclusion that the peaks close to the natural frequency of ω_0 are, in this case, masked by a residual linewidth of order precisely α_0. The Duffing oscillator contains the first two terms (effectively) of the Taylor expansion of $\cos\theta$. This numerical work by Grigolini and co-workers is equivalent to using matrices such as **M** of the order of $100\,000 \times 100\,000$ and greater. This means that convergence is, for all practical purposes, attained. In the potentials used in this paper, there are *many* intrinsic natural frequencies ω_0, and the convergence sequence illustrated in Figs. 1(c) and 1(d) would culminate in a spectrum composed of a peak for each natural frequency, each with its sequence of "satellite" peaks masked by the residual linewidth mentioned in this note. [P. Grigolini (private communication).]

ACKNOWLEDGMENTS

The University of Wales is thanked for financial support. Professor P. Grigolini, Dr. B. Zambon, Dr. M. Leoncini, Dr. M. Ferrario, Dr. S. J. Abas, Dr. F. Marchesoni, Dr. C. J. Reid, and Dr. G. J. Evans are thanked for fruitful discussions. Dr. G. J. Evans is acknowledged for a copy of his unpublished FIRRS spectrum of water, taken on a Nicolet interferometer at Warwick, U.K. Dr. C. J. Reid is thanked for a copy of his unpublished notes on the solution of Eq. (2). These notes are abstracted in this paper.

APPENDIX

If sine terms are included in the Fourier expansion for V, so that the expression for V becomes

$$V = -V_0 \sum_M \cos(M\theta) - V_0 \sum_M \sin(M\theta) \tag{A1}$$

the equivalent Kramers equation in Laplace space becomes

$$sA_r^m(s) - A_r^m(0) + \beta m A_r^m(s) + ip\alpha[A_r^{m-1}(s) + (m+1)A_r^{m+1}(s)] - i\gamma(A_{r-1}^{m-1}(s) - A_{r+1}^{m-1}) - \gamma(A_{r-1}^{m-1}(s) + A_{r+1}^{m-1}(s)) = 0 . \tag{A2}$$

It can be seen that the sine terms $[\sin(M\theta)]$ in V add real coefficients in A_{r-M}^{m-1} and A_{r+M}^{m-1} to the Kramers equation, and the cosine terms $[\cos(M\theta)]$ an imaginary part. These terms play the role of generating new peaks in the FIRRS spectrum with each new term added to the truncated Fourier-series expansion of $V(\theta)$. In theory any periodic function can be represented by a Fourier series, namely, the intermolecular functions from self-consistent field *ab initio* calculations.

[1]H. Risken and H. D. Vollmer, Z. Phys. **31B**, 209 (1978).
[2]E. Praestgaard and N. G. van Kampen, Mol. Phys. **43**, 33 (1981).
[3]H. Risken, H. D. Vollmer, and M. Morsch, Z. Phys. **40B**, 343 (1981); Mol. Phys. **46**, 555 (1982).
[4]M. W. Evans, M. Ferrario, and W. T. Coffey, Adv. Mol. Relaxation Int. Processes **20**, 1 (1981).
[5]W. T. Coffey, M. W. Evans, and P. Grigolini, *Molecular Diffusion and Spectra* (Wiley-Interscience, New York, 1984).
[6]C. J. Reid, Mol. Phys. **49**, 331 (1983).
[7]M. W. Evans, Phys. Scr. **30**, 222 (1984); Mol. Phys. **53**, 1285 (1984).
[8]G. J. Evans and M. W. Evans, J. Chem. Soc. Chem. Commun. 267 (1978).
[9]G. J. Evans and Nicolet Development Laboratories, Warwick, U.K. (private communication).
[10]G. J. Evans, J. Chem. Soc. Faraday Trans. II **79**, 547 (1983).
[11]N. N. Bogoliubov and Y. A. Mitropolsky, *Asymptotic Methods in the Theory of Non-Linear Oscillations* (Hindustan, Delhi, 1961), Chap. 3, Sec. 15.
[12]H. A. Kramers, Physica **7**, 284 (1940).
[13]S. Chandrasekhar, Rev. Mod. Phys. **15**, 1 (1943).
[14]M. W. Evans, G. J. Evans, W. T. Coffey, and P. Grigolini, *Molecular Dynamics* (Wiley-Interscience, New York, 1982).
[15]Memory Function Approaches to Stochastic Problems in Condensed Matter, two volume special issue of Advances in Chemical Physics, Vol. I, edited by M. W. Evans, P. Grigolini, and G. Pastori-Parravicini (series edited by I. Prigogine and S. A. Rice) (Wiley-Interscience, New York, in press).
[16]M. W. Evans, Phys. Rev. A **31**, 3947 (1985).
[17]M. W. Evans, C. J. Reid, S. J. Abas, and G. J. Evans, Phys. Scr. (to be published).
[18]R. P. Davies, Disc. Faraday Soc. **48**, 181 (1969).